



## Molecular Crystals and Liquid Crystals

Publication details, including instructions for authors and subscription information:  
<http://www.tandfonline.com/loi/gmcl16>

### Study of Sections of Polymerized Liquid Crystals

Y. Bouligand<sup>a b c</sup>, P. E. Cladis<sup>a d</sup>, L. Liebert<sup>a</sup> & L. Strzelecki<sup>a</sup>

<sup>a</sup> Physiques des Solides, Université de Paris-Sud, 91-Orsay, France

<sup>b</sup> Laboratoire de Zoologie, E.N.S., 46 rue d'Ulm, 75005, Paris, France

<sup>c</sup> Dept. of Zoology, Bristol, England

<sup>d</sup> Bell Laboratories, Murray Hill, New Jersey, 07974, U.S.A.

Version of record first published: 29 Aug 2007.

To cite this article: Y. Bouligand, P. E. Cladis, L. Liebert & L. Strzelecki (1974): Study of Sections of Polymerized Liquid Crystals, *Molecular Crystals and Liquid Crystals*, 25:3-4, 233-252

To link to this article: <http://dx.doi.org/10.1080/15421407408082803>

PLEASE SCROLL DOWN FOR ARTICLE

Full terms and conditions of use: <http://www.tandfonline.com/page/terms-and-conditions>

This article may be used for research, teaching, and private study purposes. Any substantial or systematic reproduction, redistribution, reselling, loan, sub-licensing, systematic supply, or distribution in any form to anyone is expressly forbidden.

The publisher does not give any warranty express or implied or make any representation that the contents will be complete or accurate or up to date. The accuracy of any instructions, formulae, and drug doses should be independently verified with primary sources. The publisher shall not be liable for any loss, actions, claims, proceedings, demand, or costs or damages whatsoever or howsoever caused arising directly or indirectly in connection with or arising out of the use of this material.

*Mol. Cryst. Liq. Cryst.*, 1974, Vol. 25, pp. 233-252  
 © Gordon and Breach Science Publishers Ltd.  
 Printed in Dordrecht, Holland

# Study of Sections of Polymerized Liquid Crystals<sup>†</sup>

Y. BOULIGAND<sup>‡</sup>, P. E. CLADIS<sup>§</sup>, L. LIEBERT and L. STRZELECKI

*Physiques des Solides  
 Université de Paris-Sud  
 91-Orsay, France*

(Received April 20, 1973)

With the polarizing microscope, we have examined thin *sections* and *polished slices* of the polymerized nematic and cholesteric mesophases. We have found that the textures we have observed are compatible with what one would expect to find in their liquid counterparts without, however, the complication of surface effects.

## INTRODUCTION

In previous works<sup>1-3</sup> we have described the synthesis of a set of new mesomorphic monomers. Their polymerization, copolymerization and terpolymerization give a new type of polymer with smectic, nematic and cholesteric structure.

In this work, we have studied the texture of copolymers from *p*-acryloyloxybenzylidene-*p*-cyanoaniline (1) and di-(*p*-acryloyloxybenzylidene)-*p*-diaminobenzene (2) (Figure. 1) and terpolymers of 1,2 and cholesterol acrylate (3).

By copolymerization, we have obtained polymers with nematic structure and by terpolymerization, the polymers with cholesteric structure.

<sup>†</sup> This work has been supported in part by the Direction des Recherches et Moyens d'Essais (Contract #71-347).

<sup>‡</sup> Permanent address: Laboratoire de Zoologie, E.N.S., 46 rue d'Ulm, 75005 Paris, France. Present address: Dept. of Zoology, Bristol England.

<sup>§</sup> Present address: Bell Laboratories, Murray Hill, New Jersey 07974, U.S.A.

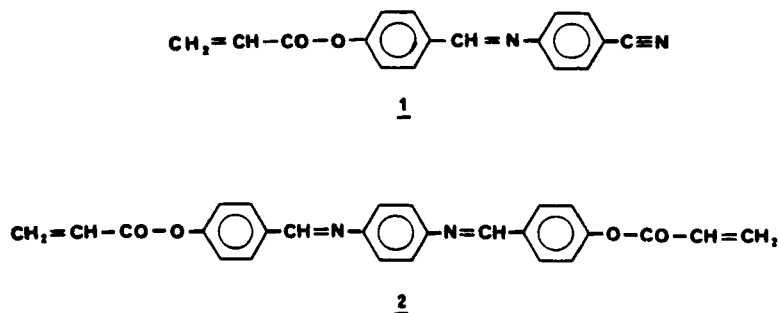


FIGURE 1 Monoacrylate monomer (shown top) and diacrylate monomer of the Schiff base.

As previously<sup>1,2</sup> all polymerizations were carried out thermally without a catalyst on a hot stage microscope between two glass slides, or in bulk, in sealed tubes.

In all cases of copolymerization the molar ratio of 1:2 has been 7:3 and in the cases of terpolymerization the molar ratio of 1:2:3 has been 7:2.75:0.25.

We have to consider these polymers as "solid-liquid crystals". In this work, we study thin sections of these polymers.

Schematic representations of reticulated nematics and cholesterics are shown in Figure 2 a and b. The reticulation process takes place in an isotropic fashion and hence the bulk optical properties of these "solid-liquid crystal" materials are identical to those of conventional liquid crystals. Since the reticulated mesophases are solid, one is able to study the optical contrast of textures which occur in bulk samples of nematics and cholesterics without the complicating factor of surface defects.<sup>4</sup> These latter are supposed to be a consequence of the anisotropy of physical parameters such as surface tension for the liquid mesophases. Evidently, one may simply remove this surface layer if the mesophase is polymerized in a solid block. The various textures may then be studied as they appear in the bulk, far from the influence of a surface. The removal of this surface layer may itself introduce artefacts which will lend their own complication to such a study. In an effort to control this, we have studied many different kinds of samples which we shall discuss in the next section.

#### Sample preparation

Our procedure was to (1) polish and (2) slice with a microtome bulk preparations of these new "solid-liquid crystals". The ultra thin sections so prepared were subsequently examined with a polarizing microscope. Frequently, we made use of the unit retardation plate ("quartz sensitive tint" or  $\lambda$ -plate) to enhance

the normally faint illumination afforded by the very thin samples between crossed polaroids.

Several kinds of samples were prepared.

A. *Polished slices* were fabricated by first sawing a slice from the bulk preparation and then polishing the parallel faces with an abrasive powder.

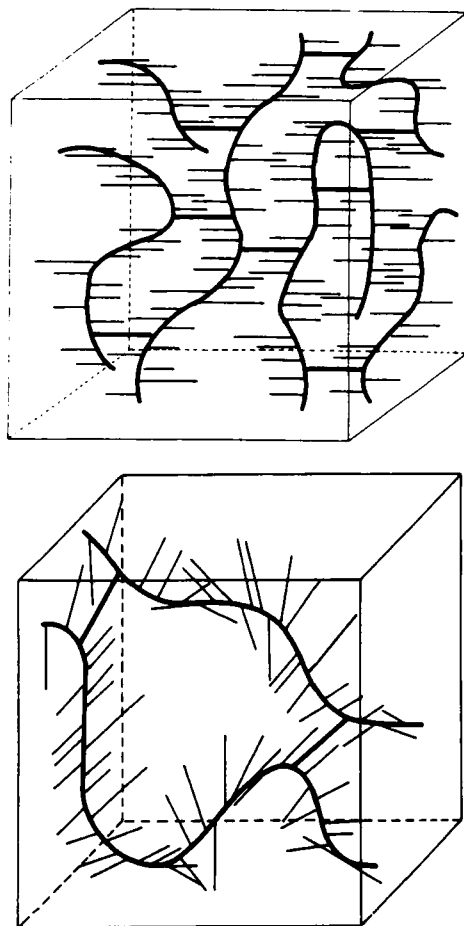


FIGURE 2 (a) A schematic representation of the reticulated nematic polymer. The macromolecules are formed at random in the three dimensional space. The lateral groups keep their initial uniaxial orientation. The copolydiacrylate molecules reticulate, yielding a solid birefringent substance. (b) A schematic representation of the reticulated cholesteric polymer. The macromolecules are formed at random in the three dimensional space. The lateral groups keep their initial twisted arrangement, typical of the liquid cholestericized nematic. The reticulated cholesteric is a *solid* birefringent substance whose optical axis is parallel to the twist axis.

B. *Thin sections* and *serial sections* were obtained by classical microtomy in use by biologists. In the case of *serial sections*, successive slices were spread on numbered slides so that the relative position of each section within the bulk sample could be reconstructed. In some cases, the serialized slices were not successive but were separated by 5 to 15 intervening slices. This enabled one to study in depth the arrangement of singularities which varied slowly over relatively large distances.

C. *Transition samples* will refer to thin samples polymerized near the isotropic transition temperature between parallel glass plates. The sample surface is left intact. Near the isotropic transition, we believe the effects of the glass surface to be negligible and that the true boundary layer is a thin layer of isotropic fluid between the glass and the remaining mesophase. The response of the mesophase to an isotropic liquid layer leads to clearer and more regular Schlieren textures. This is perhaps due to the fact that even though there are well defined (and possibly unique) conditions which must be fulfilled at the mesophase-isotropic boundary, the liquid-liquid interface can easily deform to fulfill these conditions. By comparing the optical contrast between these samples and *polished slices* or *thin sections*, one is able, in principle, to separate surface effects from bulk effects.

## Results

### A. Polymerized nematics

#### 1. $n = \pm 2$ nuclei or disclinations of strength $S = \pm 1$ <sup>†</sup>

*Thin sections* and *polished slices* of polymerized nematics may show points where the director lies perpendicular to the sample surfaces. Here, we are interested in the case where the director field around such points, as projected onto the sample surface, corresponds to that of the  $\pm 2$  nuclei (see, for example, Ref. 7). In *polished slices* or *thin sections* of polymerized nematics where the disclination line is perpendicular (or nearly so) to the exposed faces the birefringence increases slowly from zero at the center of the nucleus (where the optical axis (director) is vertical) to a maximum far from the center of the nucleus (Figure 3a). Tilting the section slightly with respect to the microscope

---

<sup>†</sup> Apparently the  $S$  designation originated with O. Lehman<sup>5</sup> and predates the nuclei or " $n$ " notation introduced by G. Friedel<sup>6</sup> and adopted by Frank.<sup>7</sup> Even nuclei ( $n = \pm 2, \pm 4$ , etc.) is synonymous with integral  $S$  (i.e.,  $S = n/2$ ) and odd nuclei ( $n = \pm 1, \pm 3$ , etc.) with half integral  $S$ . Generally in this paper we will use the nuclei notation and "even" nuclei will refer specifically to  $n = \pm 2$  and "odd" nuclei to  $n = \pm 1$  only.

axis (see Figure 3a, b) results in shifting the position of zero birefringence and hence apparently the nucleus (see Figure 4a). This was found not to be the case for the even nuclei examined in *transition samples*. For these samples, the  $\pm 2$  nuclei were very sharply defined, i.e., the birefringence decreased to zero in a relatively small distance around the nuclei. The concentrated aspect of the nucleus itself is related to the existence of singular points of the Meyer type<sup>8</sup> at the top and bottom surfaces of the sample (see Figure 3f, h). Slightly tilting the *transition samples* did not result in a marked shift of the nucleus position (Figure 4b).

Examining *polished slices* of nematics in which the polished faces were not perpendicular to the disclination line enabled us to verify the relation between "thick threads" and the even nuclei<sup>9,10,16</sup> previously pointed out by G. Friedel over half a century ago.<sup>6</sup> In a given sample one may find thick threads of different lengths corresponding to different angles between the thread (line) and the parallel faces of the sample—the longer the thread, the larger the angle. At either end of the threads, two brushes (or extinction zones where the director is either parallel or perpendicular to the polarizer or analyzer) are seen: thus, per thread, the total number of brushes is four as one expects for even nuclei. As the length of the thread decreases to zero, one finds the classical contrast of their liquid counterparts.

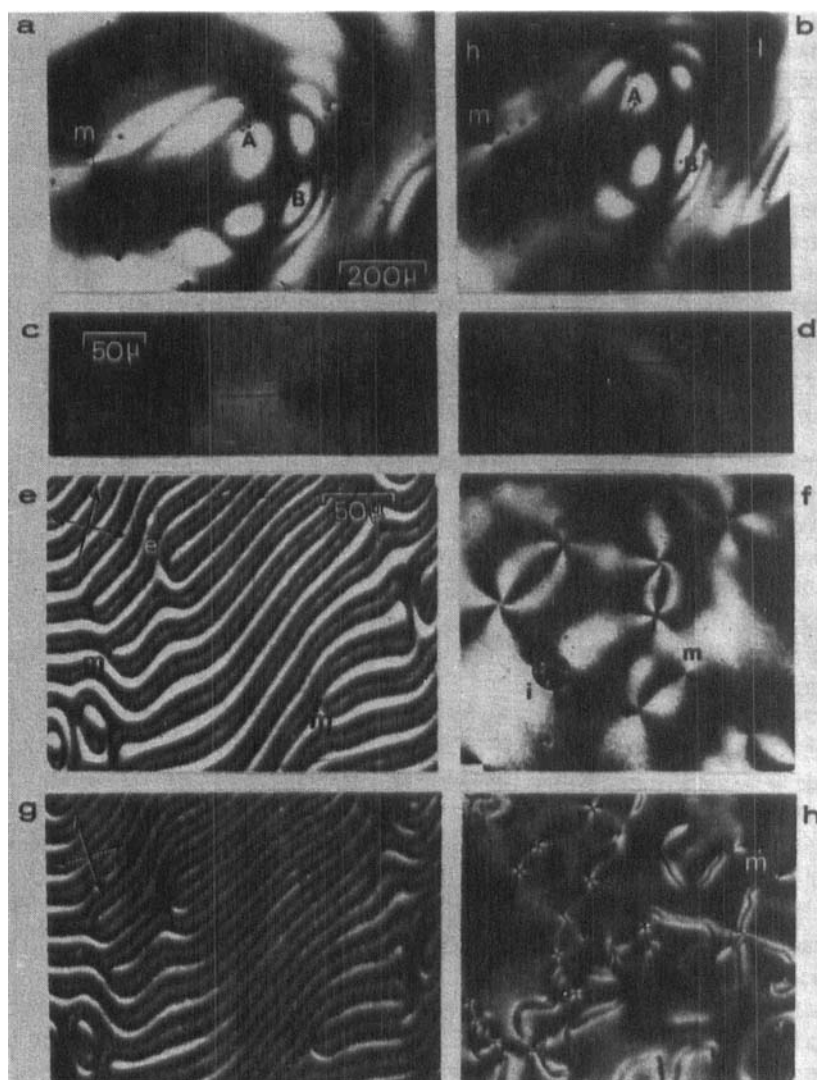
## 2. $n = \pm 1$ nuclei or $S = \pm \frac{1}{2}$

For the  $\pm 1$  nuclei, the same optical contrast is seen in *polished slices* and *transition samples* as one finds for liquid samples between glass and cover slip. In the polymerized nematics, we were able to verify the relation between the thin threads of G. Friedel and the odd nuclei (Figure 3c, d). A curiosity of some of the thin threads seen in *polished slices* is the zigzag appearance of the line seen in Figure 3d. This appears not to be an artefact arising from polishing, but may be due to the reticulation process, since it does not appear to be a feature of liquid samples.<sup>10</sup>

Tilting the sample had little or no effect upon the relative position of the odd disclination indicating that most of the changes in the director orientation takes place in a concentrated region (core) around the nuclei.

When a *transition sample* shows the homoetropic boundary condition, or only when molecules are strongly oblique, one sees bright lines connecting the odd nuclei (Figure 3h) between crossed polaroids. The birefringence in the vicinity of the bright lines is relatively large compared to the surrounding mesophase.<sup>11</sup> Furthermore, the phase contrast microscope shows these lines as ribbons stretched between the top and bottom boundaries of the mesophase. The significance of the ribbons is that they indicate the locus where the director lies parallel to the preparation surfaces. The edges of the ribbons are strongly contrasted indicating that the refractive index changes abruptly to assume the

strongly oblique or perpendicular orientation very close to the sample surface. Consequently, we suppose that the bright line arises from this abrupt change near the sample surface. Removing this layer, as we have done in the case of *polished slices* then should lead to the disappearance of the bright line. This appears to be the case (see Figure 3c, d) since we have never observed such bright lines in polished slices.



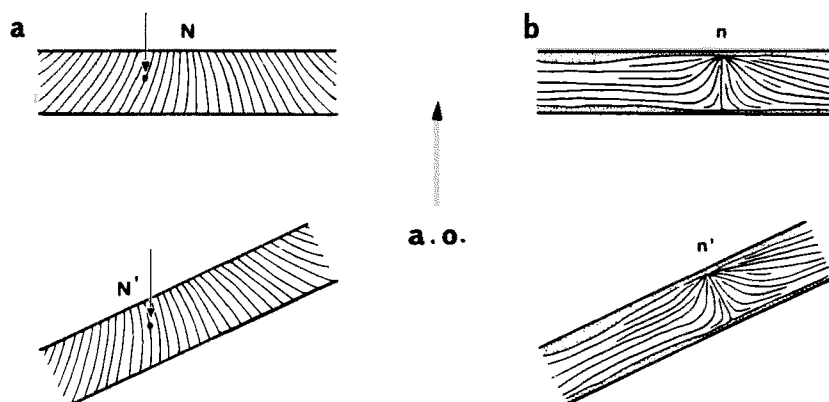


FIGURE 4 (a) Interpretation of the tilting effect of an even nucleus in a *polished slice*. The center of the nucleus appears at  $N$  where the molecules lie mainly parallel to the optical axis, o.a. When the slice is tilted, the nucleus is shifted to  $N'$ . (b) Even nuclei in *transition sample* are more sharply defined due to the presence of point singularities at the sample surface. Tilting these samples does not result in a marked shift of the nucleus position.

FIGURE 3 All the samples are examined between crossed polaroids. (a) A *polished slice* in the vicinity of an even nucleus.  $A, B, C$  are impurities in the sample;  $m$  is an odd nucleus corresponding to an almost vertical thin thread. (b) The effect of tilting the slice with respect to the microscope axis by an angle of about  $25^\circ$  is to shift the center of the Maltese cross of the nucleus with respect to three fixed points  $A, B, C$  in the sample.  $h$  and  $l$ : high and low levels in the tilted view. (c,d) A *polished slice* of nematic showing the relation between the thin threads of G. Friedel and the odd nuclei. Note the zigzag appearance of the thin thread in (d). The nucleus in (c) corresponds to a  $-\pi$  disclination and to a  $+\pi$  disclination in (d). The zigzag appearance may occur in both  $+$  and  $-\pi$  disclinations. (e.g.) Thin sections of a polymerized cholesteric.  $e$  is an edge dislocation which effects a change in the number of dark double lines by two (i.e. one helical pitch). The two types of contrast for the edge dislocation  $e$  depend upon the orientation of the projected twist axis with respect to the crossed polaroids represented by double arrows.  $m$  are edge dislocations which effect a change in the number of dark double lines by one (i.e. a half pitch). Note the odd nuclei at these levels. (f) A *transition sample* in a nematic. Even nuclei (e) from Maltese crosses and odd nuclei (m) show only two dark branches. (i) is an isotropic area where some polymerized mesomorphic droplets can be seen. (h) A *transition sample* with boundary conditions leading to particularly bright lines surrounding some even nuclei and linked to the odd nuclei (m). Same scales for (a) and (b); another scale for (c), (d), (f), (h) and a different one for (e) and (g).

### B. Polymerized cholesterics

From the classical works of Grandjean and Friedel<sup>6,12</sup> we recall that for smectics and cholesterics, the parallel layers form cones of revolution nested along curves which are conics (the focal hyperbolas, ellipses or parabolas, see Figure 5). The layers are not peaked at the cone top but rather, rounded off, i.e. the curvature of the cone surface is well-defined everywhere including the cone peak. It has recently been shown<sup>13</sup> that these nested layers are not always exactly figures of revolution and that curves along which they are stacked are not necessarily conics. We shall call these curves rather "focal lines". They are the locus of the maximum of the mean curvature of the layered surfaces.

Focal lines can be found in *thin sections* of cholesteric polymers. When the plane of section lies almost perpendicular to the focal line, one observes, between crossed polaroids, concentric rings. Upon rotating the microscope stage, one witnesses the famous moving fringes of the liquid crystal pioneers.<sup>12</sup>

When the section planes are slightly inclined with respect to the focal line, the curvature of the periodically alternating dark and bright lines shows a strong maximum at a point *A* (see Figure 5a, b) where the focal line meets the section plane. The focal line can be followed on *serial sections* and the relative position of the point *A* shifts from section to section (see Figure 5a, b). As can be seen from the photos, the relative position of *A* can be determined by its location with respect to dislocations which lie almost perpendicular to the cutting plane. The periodicity of the cholesteric is evidently minimum around the dislocations.

We have observed numerous examples of edge dislocations formed by disclinations of opposite signs:

- 1) Groups of four disclinations, two  $+\pi$  and two  $-\pi$  give prisms with a lozenge or parallelogram base (see Figure 5c-g) which can be followed on serial sections. Sometimes the lozenge shape is not very regular. Such patterns have been frequently observed in the fan shaped texture<sup>13</sup> of liquid cholesterics.

- 2) Edge dislocations which effect a change in the number of dark lines by one (i.e. a change of half of a pitch) show a definite odd nucleus (see *m* in Figure 3e, g) with a core region. On the other hand, those which introduce two new lines (corresponding to a change of a whole pitch) do not exhibit such contrast (see *e* in Figure 3e, g). The question of contrast for the cholesterics will be discussed further in the next section.

- 3) The final observation we would like to list here concerns the optical contrast of the edge dislocation. We found two types of contrasts depending upon the relative orientation of the projected twist axis with respect to the polarizer and analyzer (see *e* in Figure 3e, g).

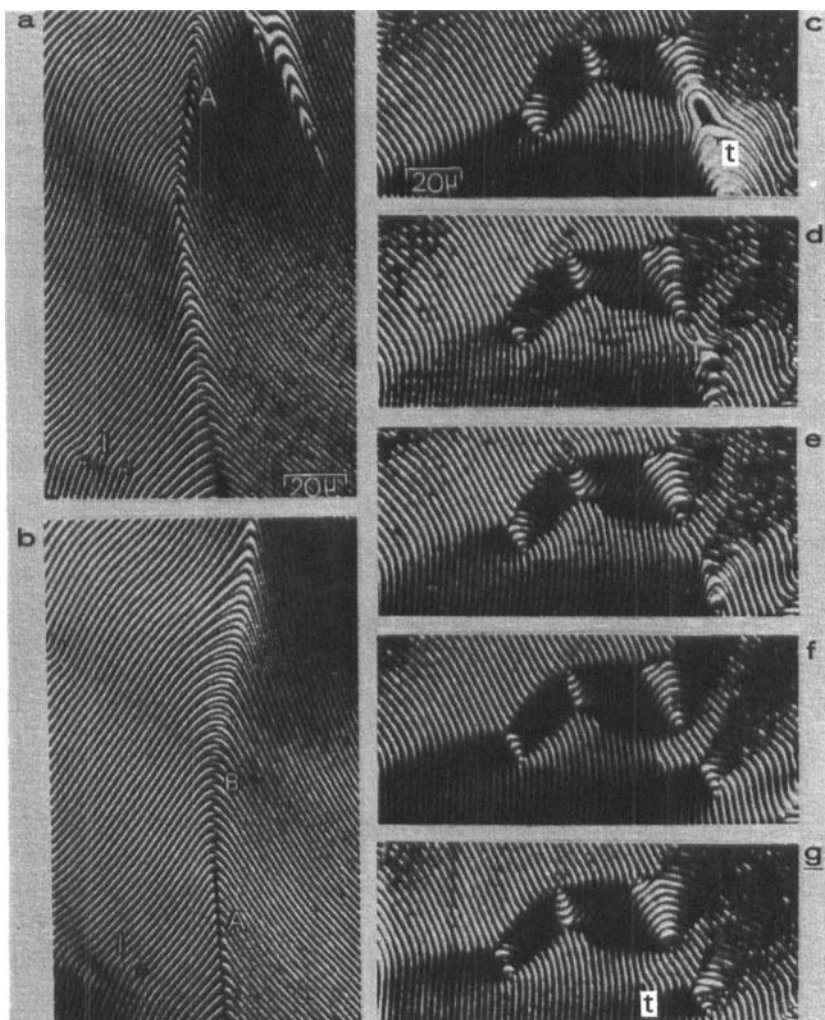


**FIGURE 5** All the samples are examined between crossed polaroids. (a,b) Serial sections taken along a focal line. The maximum of curvature in the alternating dark and bright lines occurs where the section plane passes closest to the focal curve or crosses it. The peak of the nested cones of Grandjean and Friedel are rounded off along the focal curve along which they are stacked. When a polymerized cholesteric is sectioned in a plane nearly parallel to the focal plane and which includes the point *A*, one sees a strong maximum in the curvature of the twist axis at the point *A*. The further away the section plane is to the focal line the smaller the curvature. The level *A* is shifted from one section (a) to another (b) with respect to the dislocation designated as *I* in (a) and (b). At *B*, single dark lines branch into two (see Figure 12). (c,g) Parallelogram shapes formed by disclinations. *Serial sections* show that the disclinations form prisms in space. *t* is a translation dislocation (probably a screw-dislocation). Scales are the same in (a) and (b); another scale for (c-g).

## Discussion

### A. Nematic samples

The "mobility" of the even nuclei upon tilting the polished slices (Sec. 3—A.1) is related to their coreless character.<sup>9,14,15</sup> In the bulk, the director field around even nuclei is planar only very far from the nuclei (or line). The closer the distance to the nucleus, the larger the vertical component (or component parallel to the line). This change, however, takes place relatively slowly (on a macroscopic scale) so that the elastic energy never exceeds the limits of linearized elasticity, i.e. the Frank equation.<sup>7</sup>

Taking the line to be along the  $z$ -axis, the director field in cylindrical coordinates is

$$\begin{aligned} n_r &= \cos(\alpha\theta - \delta) \cos \varphi(r, z) \\ n_\theta &= \sin(\alpha\theta - \delta) \cos \varphi(r, z) \\ n_z &= \sin \varphi(r, z) \end{aligned} \quad (1)$$

where  $r = \sqrt{x^2 + y^2}$  is the distance from the line in a plane perpendicular to it,  $\tan \theta = y/x$ ,  $\delta$  is a constant,  $\varphi$  is the angle between  $n$  and the  $x$ - $y$  plane and  $(1 + \alpha)S = n/2$ , where this last  $n$  refers to the nuclei notation not the director. In the one constant limit (the elastic constants of splay ( $k_{11}$ ), twist ( $k_{22}$ ) and bend ( $k_{33}$ ) all equal to  $k$ ), the Frank equation is

$$\begin{aligned} \frac{2f}{k} = & \left[ \frac{(1+\alpha)^2 \cos^2 \varphi}{r^2} - \frac{2(1+\alpha)}{r} \frac{\partial \varphi}{\partial r} \cos \varphi \sin \varphi + \left( \frac{\partial \varphi}{\partial r} \right)^2 + \left( \frac{\partial \varphi}{\partial z} \right)^2 \right. \\ & \left. + \frac{2(1+\alpha)}{r} \frac{\partial \varphi}{\partial r} \cos^2 \varphi \cos(\alpha\theta - \delta) \right] \end{aligned} \quad (2)$$

and the Euler-Lagrange equation is

$$r \frac{\partial}{\partial r} r \frac{\partial \varphi}{\partial r} + r^2 \frac{\partial^2 \varphi}{\partial z^2} = -(1+\alpha)^2 \cos \varphi \sin \varphi. \quad (3)$$

The case  $S = \pm 1 = (1+\alpha)$  and  $\partial \varphi / \partial z = 0$  has been extensively discussed elsewhere.<sup>9,14</sup>

1) When  $\partial \varphi / \partial z = 0$  we note from (3) the odd nuclei also have a non-planar solution, i.e.

$$\left( \frac{R_{\max}}{r} \right)^{\pm \frac{1}{2}} = \tan \left( \frac{\pi}{4} + \frac{\varphi}{2} \right) \quad (4)$$

for which  $\varphi = \pi/2$  at  $r = 0$ . However, as pointed out in Ref. (14) and is not evident from (4), is that such a solution introduces a discontinuity in the direc-

tor field along the plane  $\theta = 0$ . The energy of this discontinuity must be added to (2) to obtain the total energy of such a configuration.

2) We consider the case  $\partial\varphi/\partial z \neq 0$  for infinite samples with cylindrical symmetry. Then a solution for (3) is

$$\ln \tan\left(\frac{\pi}{4} + \frac{\varphi}{2}\right) = \pm |1+a| \ln\left(\frac{z}{r} + \sqrt{\frac{z^2}{r^2} + 1}\right). \quad (5)$$

This can be deduced quite simply by supposing  $\varphi(u)$  only where  $u = z/r$ . In the case  $|1+a| = 1$ , this can be more simply expressed as

$$\tan \varphi = \pm z/r \quad (6)^\dagger$$

Eq. (6) is illustrated in Figure 6. For the odd nuclei, we have

$$\begin{aligned} \cos \varphi &= \pm \left( \frac{2r}{r + \sqrt{r^2 + z^2}} \right)^{\frac{1}{2}} \\ \sin \varphi &= \frac{z}{r + \sqrt{r^2 + z^2}} \end{aligned} \quad (7)$$

As in Sec 1 above, we find the appearance of a surface discontinuity for the odd nuclei as well as the singular point at  $z = r = 0$ . We note in Eq. (7) that for a given sign of  $z$ ,  $\cos \varphi$  may be either positive or negative.

3) We now wish to present a topological extension of the above considerations for the transition samples. For these samples, we put  $\varphi = 0$  at  $z = 0$  and  $\varphi = \pi/2$  at  $z = d$ .

a) For the even nuclei, we assume a solution to Eq. (3) exists for which  $\tan \varphi(r, d) = \infty$  and  $\tan \varphi(r, 0) = 0$ . The simplest such solution is likely to be of the form indicated in Ref. 8. Thus, in a bounded geometry, even nuclei require a point singularity to satisfy the above boundary conditions.

b) For the odd nuclei, we suppose that we may smooth out the surface discontinuity (e.g. by introducing a  $\theta$  dependence for  $\varphi$ ) in the bulk of the sample. We arrive at the scheme drawn in Figure 7 where we see that in this model the odd nuclei in a bounded geometry require a line singularity near one surface,  $z = d - \eta$ , as well as a point singularity at  $z = 0$ . This is exactly analogous to the case of cholesterics as discussed in Ref. 4. The line singularity near the surface is

---

<sup>†</sup> Solving the Euler-Lagrange in spherical coordinates, Saupe(17) has found many more types of point singularities including these.

of the planar odd nuclei type, therefore requires a core. It may be of either sign depending upon the sign of  $\partial\phi/\partial z$ . For the boundary conditions given, it will lie below (or above) a region where the birefringence of the sample is maximum. In this model, the extraordinary rays will tend to follow a path curved towards the surface line and hence contribute to an enhancement of the intensity in the vicinity of the line.

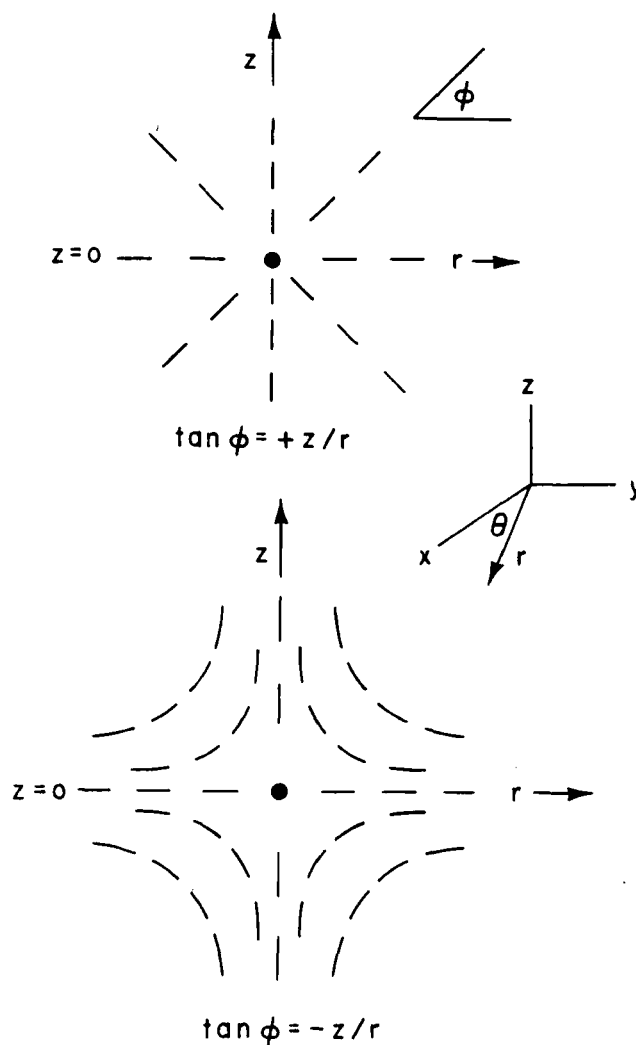


FIGURE 6 Solution to Eq. 3 for infinite samples  $|1+\alpha|=1$ .

To sum up then, we have assumed that we may apply these conclusions for liquid nematics to their polymerized counterparts. In transition samples, where we observe surface as well as bulk deformations we have seen that even nuclei require at least one point at a surface to satisfy a given boundary condition (Figure 6). Whereas the odd nuclei require a singular surface line as well as a point to satisfy the same boundary conditions (Figure 7). We attribute the bright

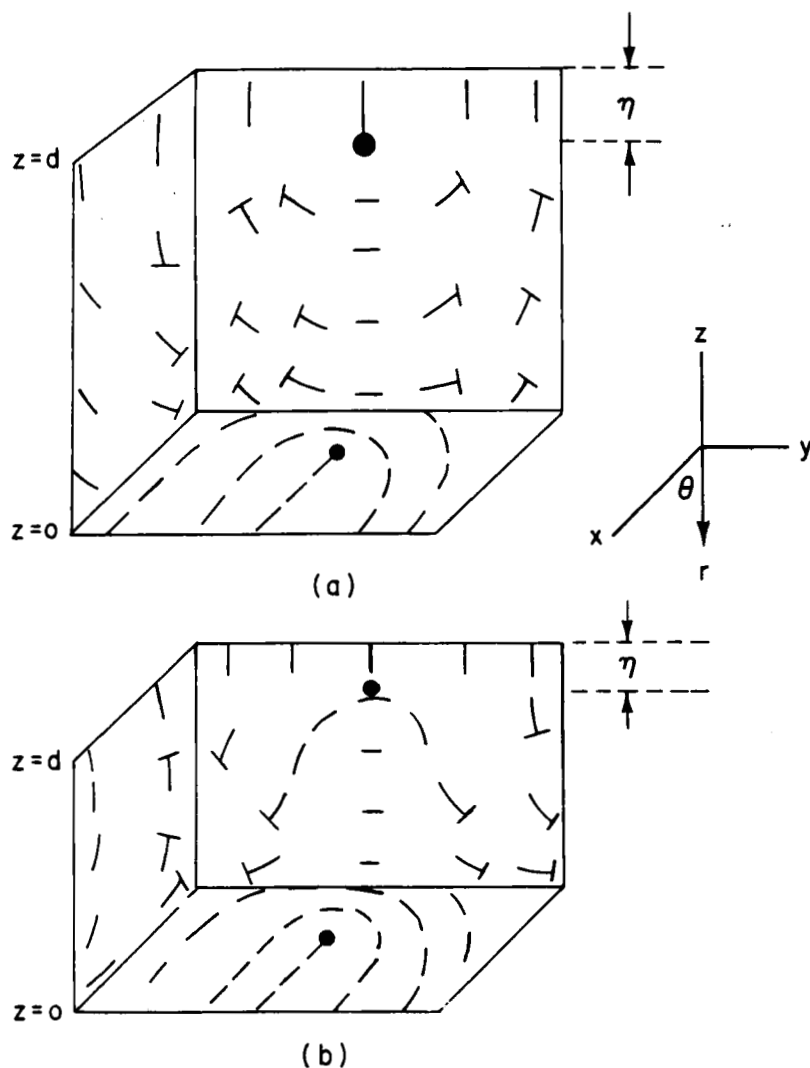


FIGURE 7 (a) Non-planar configurations for the odd nuclei lead to a line singularity running parallel to surface as well as the point at  $r = z = 0$ . The cube is viewed from below.

line commonly seen linking odd nuclei in transition samples to this surface line. The surface points and lines both require core regions<sup>†</sup> which have optical parameters enabling one to distinguish them from the rest of the sample. Their apparent position, then, will not be dependent upon the direction from which they are viewed. Further discussions<sup>13</sup> will show that in nematic liquid crystals, in slightly cholesteric mesophases and in their polymerized counterparts, the boundary conditions can be more sophisticated. In many cases, it appears that two angles  $\varphi_1$  and  $\varphi_2$  are defined and one has

$$0 \leq \varphi_1 \leq \varphi \leq \varphi_2 < \pi/2. \quad (8)$$

The left inequalities lead to superficial singular lines whereas the right inequalities give rise to singular points.

In polished slices, the surface layer is removed. We still observe a core region for the odd nuclei (Figure 3c, d) but no longer for the even nuclei which, not requiring cores in the bulk, are no longer "fixed" in space by surface point defects (Figure 3a, b).

### B. Cholesteric samples

In Figure 8, we show a schematized  $+\pi$  disclination viewed with the twist axis in the plane of the figure (plane  $P$ ). Projecting this configuration onto a plane tilted with respect to it by an amount  $\pm\alpha$  (planes  $S_1$  and  $S_2$  of Figure 8d and f) results in the configuration shown. Here we show only the projection of the director onto the  $S$  planes. These show the typical bow-shaped curves or "arceau" of a "tilted" cholesteric (Figure 8c, e). The component of the director out of the plane is not shown. This is a maximum at the peak of the bow and a minimum at the ends of the bow (see Figure 8). Aspects of disclinations  $+\pi$  and  $-\pi$  are given on Figure 9a-d.

In Figure 9e, f and Figure 11 we show the edge dislocation which results when a (tilted) positive  $\pi$  disclination is combined with a (tilted) negative  $\pi$  disclination. The resulting optical contrast is shown in Figure 10b and c. The dark lines in Figure 10 indicate where extinction would occur for the position of the polarizer and analyzer indicated. We see that there are, in fact, two types of patterns to be expected and that these correspond quite well with what we have observed in Figure 3e, f.

---

<sup>†</sup> One can also imagine that the effect of the surface defects is to deform the surface. This would also create an optical effect which is independent of the inclination of the sample. This would be an interesting possibility to pursue in a later study.

In Figure 12 we wish to discuss the contrast given by one half pitch of a cholesteric for a given setting of the crossed polaroids. The stippled region represents zones which are extinguished. When the projected twist axis is parallel to either a polarizer or an analyzer, we expect extinction in two regions: (1) the region between bows ( $B$  on Figure 12) and (2) at the peak of the arceau ( $A$  on the figure). As the projection of the twist axis "turns the corner", we expect the  $B$  lines to move in towards the arceau peak as the  $A$  lines

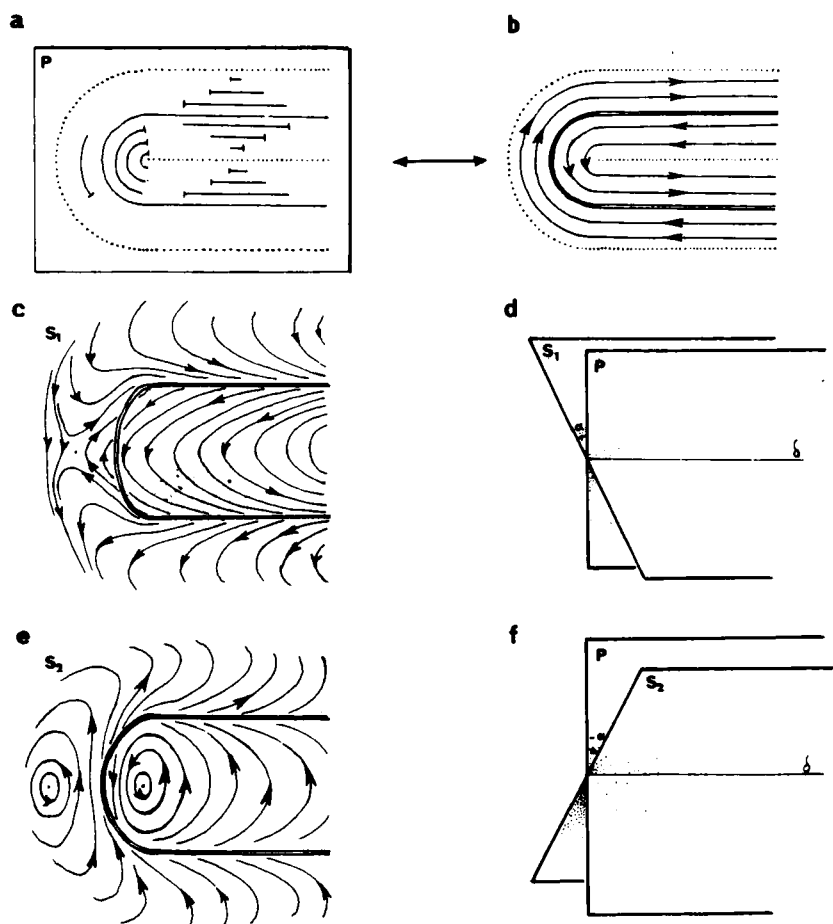


FIGURE 8 (a) A schematized  $+\pi$  disclination viewed with the twist axis in the plane  $P$  of the figure. An alternative representation is given in (b). In (c) and (e), we show the projection of this configuration onto the section planes  $S_1$  and  $S_2$ , shown in (d) and (f). The straight lines  $\delta$ , where  $S_1$  or  $S_2$  intersect  $P$ , are here taken to be parallel to the horizontal plane of symmetry of the disclination. The more general case is shown in Figure 9.

move towards the region between bows. When these two lines straddle a bow peak, a single dark line is expected to result. This is due partly to the fact that the peak of the bow corresponds to a region for which the birefringence is smallest (the director here having its maximum tilt out of the sample plane) and partly due to an artefact arising from the slicing technique which enhances the curvature of the bow (see Figure 13). This last effect leads to the *B* and *A* lines being closer together and hence, much less distinguishable when the projection of the twist axis is at 45 degrees to the crossed polaroids than when it lies along either a polarizer or analyzer. Thus, we have the phenomenon of a single dark

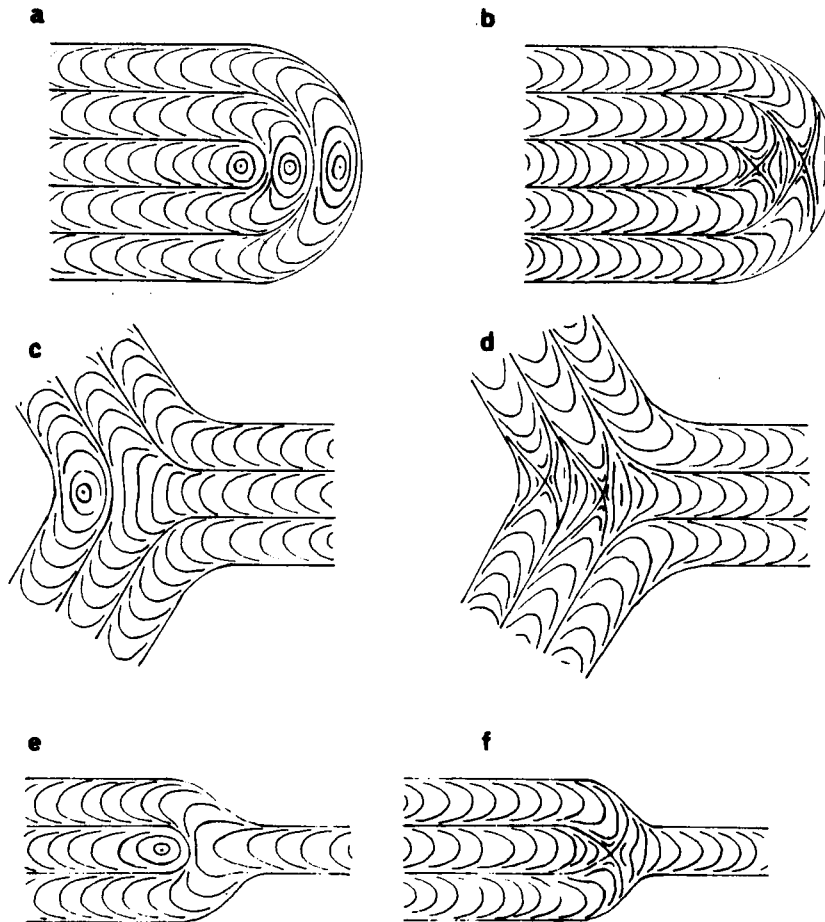


FIGURE 9 (a,b,c,d) Aspects of disclinations given by oblique section planes as in the preceding figure. (e,f) The edge dislocation which results when a positive-disclination (shown in a or b) is combined with a negative  $\pi$  disclination (shown in c or d).

line branching into two dark lines as the projected twist axis "turns a corner". This is illustrated in Figure 5a, b.

## CONCLUSIONS

A) The textures we have observed in the polymerized liquid-crystals are quite compatible with what one would expect from the liquid mesophases without, however, the complication of surface effects.

B) In the case of the nematic polymers:

1) We have been able to verify the relation between the thick and thin threads of G. Friedel and the even and odd nuclei (Figure 3c, d).

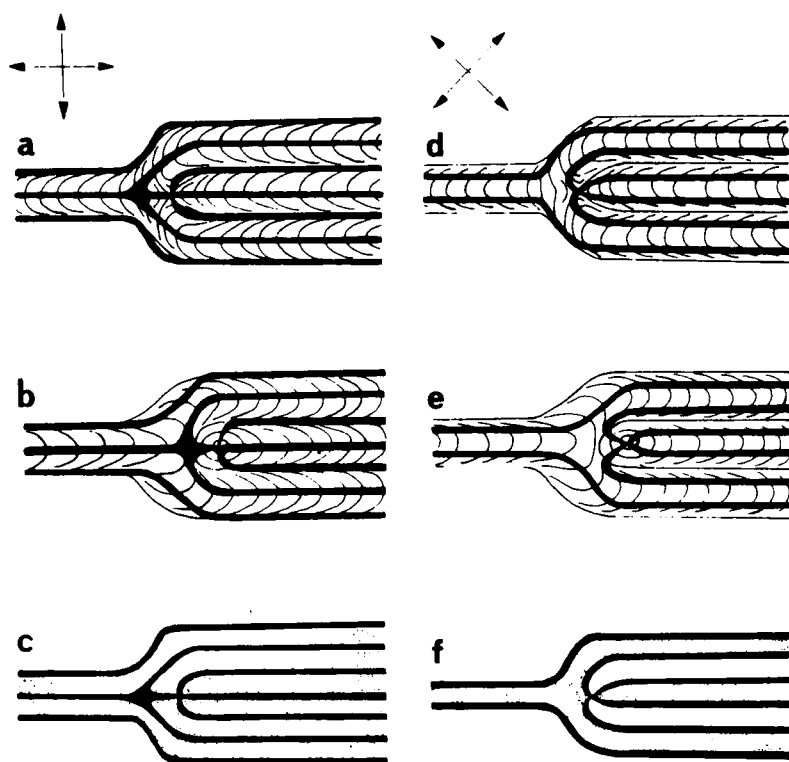


FIGURE 10 The optical contrast of Figure 9f is shown in Figure 10a, d for two different settings of the crossed polaroids. Figure 9e is shown in Figure 10b, e. The contrast in (a) and (b) are similar and lead to the picture given in (c); (d) and (e) lead to (f). The contrast of an even edge dislocation depends upon the orientation of the crossed polaroids.

2) We have seen that the position of the non-singular even nuclei apparently shifts when the sample preparation is slightly tilted with respect to the microscope axis (Figure 3a, b). This tilt dependence was not observed on singularities with core regions (Figure 3f, h).

3) The bright lines often found linking odd nuclei in liquid samples were not found to be present in *polished slices* (Figure 3a-d) whereas they were found to be present in some *transition samples* (Figure 3h) thus supporting the hypothesis that the bright line is due to surface effects.

C) In the case of polymerized cholesterics:

1) We have verified the existence of the two possible contrasts for an edge dislocation (Figure 3e, g and 10c, f).

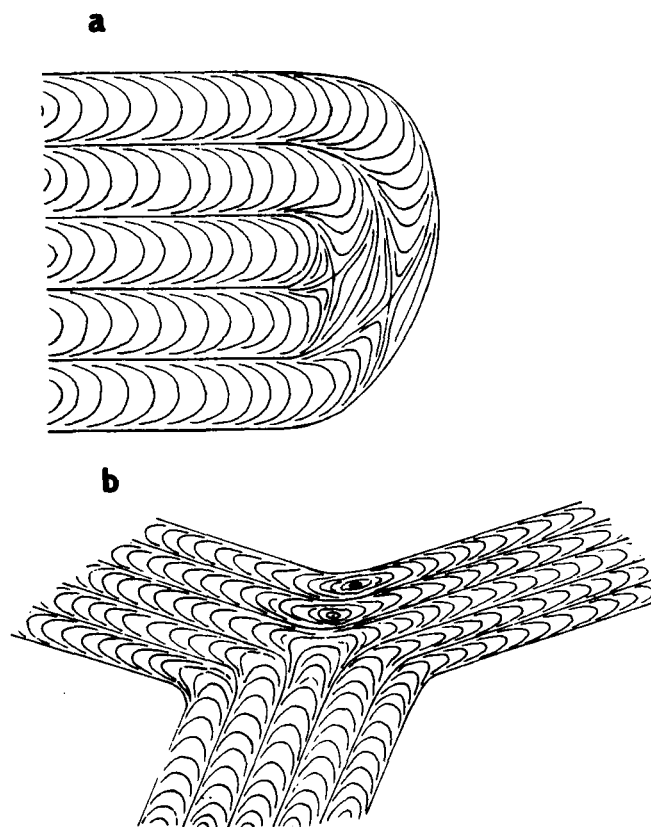


FIGURE 11 Here, we show the general case (corresponding to Figure 8), where the projection plane  $S$  cuts the plane  $P$  in an arbitrary direction,  $\delta$ .

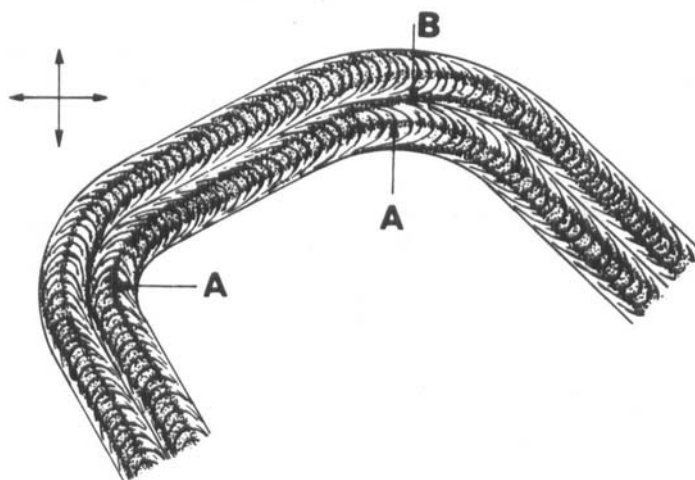


FIGURE 12 The contrast shown by two bow shaped series (one pitch), for which the twist axis is tilted out of the plane of the figure. The stippled regions represent zones of extinction for the given setting of crossed polaroids. Some extinction is also expected at the arceau peaks where the birefringence is smallest (the director here having its maximum tilt out of the sample plane). The phenomenon of a single dark line branching into two dark lines can be seen in Figure 5b at *B*.

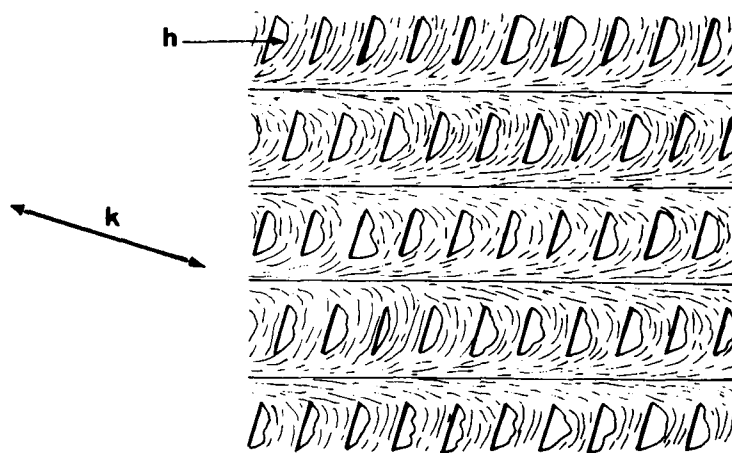


FIGURE 13 The effect of slicing the cholesteric is to distort the bow-shaped patterns in the direction of cutting *k*. Regularly ordered holes can appear in the section as seen on the right of Figure 5c, g.

2) We have also seen that the phenomenon of a single dark line branching into two dark lines as the projected twist axis "turns a corner" is compatible with what one would expect from a "tilted" cholesteric (Figure 3e, g; 5a, b and Figure 12) for a given setting of the crossed polaroids.

3) The edge dislocation required to change the number of pitches by one half a pitch has been found to show a definite odd nuclei with a core region as one would expect from topological considerations (m in Figure 3e, g).

4) In *serial sections* we have been able to follow a focal line in depth thus verifying their existence (Figure 5a, b).

### References

1. Strzelecki, L. and Liebert, L., *Bull. Soc. Chem. F.*, 597 (1973).
2. Liebert, L. and Strzelecki L., *ibid*, 603 (1973).
3. Strzelecki L. and Liebert, L., *ibid*, 605 (1973).
4. Cladis, P. E. and Kleman, M., *Mol. Cryst. and Liq. Cryst.* 16, 1 (1972).
5. We are indebted to J. Nehring for this remark.
6. Friedel, G., *Ann. Phys. Paris* (9) 18, 273 (1922).
7. Frank, F. G., *Disc. Faraday Soc.* 25, 19 (1958).
8. Meyer, R. B., *Mol. Cryst. and Liq. Cryst.* 16, 355 (1972).
9. Meyer, R. B., *Phil. Mag.* 27, 405 (1973).
10. Bouligand, Y, (to be published).
11. Nehring, J, and Saupe, A., *J. Chem. Soc., Faraday Trans. II*, 68, 1 (1972).
12. Grandjean, F., *C. R. Acad. Sci. Paris*, 172, 71 (1921).
13. Bouligand, Y, (to be published).
14. Cladis, P. E. and Kleman, M., *J. de Physique* 33, 591 (1972).
15. Williams, C. E., Pieranski, P. and Cladis, P. E., *Phys. Rev. Letters* 29, 90 (1972).
16. Nehring, J., *Phys. Rev. Rev.* 7, 1737 (1973).
17. Saupe, A., presented at the Fourth International Liquid Crystal Conference, Kent, Ohio, August 1972. *Mol. Cryst. Liq. Cryst.* 21, 211 (1973).